Properties of moment tensors of sources in anisotropic media

Václav Vavryčuk

Geophysical Institute, Academy of Sciences, Boční II/1401, 141 31 Praha 4, Czech Republic.
E-mail: vv@ig.cas.cz

SUMMARY

Seismic sources in anisotropic media have more complicated moment tensors than in isotropic media. Planar shear sources produce pure double-couple (DC) moment tensors in isotropy, but generally non-double-couple (non-DC) moment tensors in anisotropy. The non-DC components can comprise both the isotropic (ISO) and compensated linear vector dipole (CLVD) components. The amount of the ISO and CLVD depends on the orientation, strength and symmetry of anisotropy. Shear sources generate no non-DC components in anisotropy, provided that shear faulting is situated in symmetry planes of orthorhombic or higher anisotropy symmetries. The fault plane solution, i.e. the orientation of the fault normal and the slip direction, can be retrieved from a moment tensor and elastic parameters describing anisotropy. Numerical modelling on media with aligned dry or water-filled penny shaped cracks shows that shear faulting generates non-DC components with the percentage comparable with strength of anisotropy. The medium with water-filled cracks produces almost no ISO components. The focal mechanisms seem to be less sensitive to anisotropy than the percentages of the non-DC components.

1. Introduction

Anisotropy is a pervasive property of geological structures in the Earth crust and in the upper mantle (Babuška & Cara 1991; Rabbel & Money 1996; Silver 1996; Savage 1999). It is caused by sediment layering, by stress-aligned systems of microcracks, cracks or fractures or by textural ordering of rock-forming minerals. Anisotropy significantly affects seismic observations: it affects propagation of seismic waves as well as generation of waves by seismic sources. So far seismologists focused mainly on studying theoretical aspects of wave propagation in anisotropic media (e.g., Helbig 1994; Červený 2001), and on observing effects of anisotropy on seismic waves (Babuška & Cara 1991) as, for example, a spatial variation of seismic velocities or the shear-wave splitting, detected and measured in situ at regional or local scales (Kaneshima et al. 1988; Crampin 1993) or in the laboratory on rock samples (Kern & Schmidt 1990; Pros et al. 1998; Mainprice et al. 2000). However, equally important point is how anisotropy affects generation of seismic waves. For example, Kawasaki & Tanimito (1981) point out that a shear source in an anisotropic medium can generate a moment tensor, which is not pure double couple (DC), and nodal lines, which display peculiarities not observed in isotropic media. Since the non-double-couple (non-DC) components of moment tensors are frequently observed for earthquakes (Sipkin 1986; Kuge & Kawakatsu 1992; Kuge & Lay 1994; Miller et al. 1998), the problem, whether anisotropy contributes to them or not, is not only of theoretical interest but also of practical relevance. Anisotropy as a possible cause of non-DC components of moment tensors has been mentioned and discussed also by other authors (Kawakatsu 1991; Frohlich 1994; Julian et al. 1998; Vavryčuk 2002; Rössler et al. 2003). Since the effects of anisotropy on seismic sources are not so far well understood, we present a detailed mathematical description of the problem in this paper. We define conditions under which shear faulting in anisotropic media can be represented by pure double couple and describe a procedure how to determine geometry of faulting from moment tensors of sources situated in anisotropic media. Using synthetic media with aligned cracks, we illustrate properties of non-DC components of moment tensors in dependence on the orientation of faulting in anisotropy. We also estimate errors in the determination of nodal planes due to the neglect of anisotropy.

2. Theory

2.1. Moment tensors

2.1.1. Isotropic medium

Moment tensor **M** of a seismic source in an isotropic medium is expressed as (Aki & Richards 2002, Eq. 3.21)

$$M_{ij} = uS\left[\lambda \nu_k n_k + \mu\left(\nu_i n_j + \nu_j n_i\right)\right] , \qquad (1)$$

where u is the slip, S is the fault area, λ and μ are the Lamé constants describing the isotropic medium surrounding the fault, $\mathbf{v}$ is the slip direction, and **n** is the fault normal. For shear sources, eq. (1) further simplifies to (Aki & Richards 2002, Eq. 3.22)

$$M_{ij} = \mu u\, S\left(\nu_i n_j + \nu_j n_i\right) , \qquad (2)$$

which is the common double-couple representation of an earthquake source.

2.1.2. Anisotropic medium

The moment tensor **M** of a seismic source in an anisotropic medium is defined as (Aki & Richards 2002, Eq. 3.19)

$$M_{ij} = uSc_{ijkl}\nu_k n_l , \qquad (3)$$

where c_{ijkl} are the elastic parameters of the anisotropic medium surrounding the fault. Because of symmetry of c_{ijkl} equation (3) can be expressed as follows

$$M_{ij} = uSc_{ijkl}\frac{1}{2}\left(\nu_k n_l + \nu_l n_k\right) = c_{ijkl}D_{kl} , \qquad (4)$$

where **D** denotes a symmetric dyadic tensor

$$\mathbf{D} = \frac{uS}{2}\left(\mathbf{n}\mathbf{v} + \mathbf{v}\mathbf{n}\right) , \qquad (5)$$

called the source tensor. Equation (4) is similar to the generalized Hooke's law, but instead of the relation between the stress and strain tensors, it expresses the relation between the moment and source tensors. Equation (4) can equivalently be expressed in a matrix form as

$$\mathbf{m} = \mathbf{C}\mathbf{d}\,, \tag{6}$$

where **C** is the 6x6 matrix of the elastic parameters in the two-index Voigt notation, where subscripts are substituted in the following way: 11→1, 22→2, 33→ 3, 23→ 4, 13→ 5 and 12→ 6 (see Musgrave 1970, eq. 3.13.4). Quantities **m** and **d** are the 6-vectors defined as:

$$\mathbf{m} = \left(M_{11}, M_{22}, M_{33}, M_{23}, M_{13}, M_{12}\right)^T\,, \tag{7}$$

$$\mathbf{d} = uS\left(n_1\nu_1, n_2\nu_2, n_3\nu_3, n_2\nu_3 + n_3\nu_2, n_1\nu_3 + n_3\nu_1, n_1\nu_2 + n_2\nu_1\right)^T\,. \tag{8}$$

The vector **d** and source tensor **D** are related as follows

$$\mathbf{D} = \frac{1}{2}\begin{bmatrix} 2d_1 & d_6 & d_5 \\ d_6 & 2d_2 & d_4 \\ d_5 & d_4 & 2d_3 \end{bmatrix}. \tag{9}$$

As seen from eq. (3) the moment tensor for anisotropic media has a more general form than for isotropic media comprising the double-couple (DC), but also the isotropic (ISO) and the compensated linear vector dipole (CLVD) components (Knopoff & Randall 1970; Jost & Hermann 1989; Lay & Wallace 1995; Vavryčuk 2001). The non-DC components (ISO and CLVD) can be non-zero even for shear earthquakes (Kawasaki & Tanimoto 1981).

2.1.3. Special cases

The moment tensor for anisotropic media can simplify for a special geometry of faulting or for special types of anisotropy. Supposing, for example, a shear source with $\mathbf{n} = (0,0,1)^T$ and $\mathbf{v} = (1,0,0)^T$, we get $\mathbf{d} = (0,0,0,0,uS,0)^T$, and eq. (6) yields for triclinic anisotropy

$$\mathbf{m} = \mathbf{Cd} = \begin{bmatrix} C_{11} & C_{12} & C_{13} & C_{14} & C_{15} & C_{16} \\ & C_{22} & C_{23} & C_{24} & C_{25} & C_{26} \\ & & C_{33} & C_{34} & C_{35} & C_{36} \\ & & & C_{44} & C_{45} & C_{46} \\ & & & & C_{55} & C_{56} \\ & & & & & C_{66} \end{bmatrix} \cdot \begin{bmatrix} 0 \\ 0 \\ 0 \\ 0 \\ uS \\ 0 \end{bmatrix} = uS \begin{bmatrix} C_{15} \\ C_{25} \\ C_{35} \\ C_{45} \\ C_{55} \\ C_{56} \end{bmatrix}. \qquad (10)$$

If anisotropy displays orthorhombic or higher symmetry, then

$$\mathbf{m} = \mathbf{Cd} = \begin{bmatrix} C_{11} & C_{12} & C_{13} & 0 & 0 & 0 \\ & C_{22} & C_{23} & 0 & 0 & 0 \\ & & C_{33} & 0 & 0 & 0 \\ & & & C_{44} & 0 & 0 \\ & & & & C_{55} & 0 \\ & & & & & C_{66} \end{bmatrix} \cdot \begin{bmatrix} 0 \\ 0 \\ 0 \\ 0 \\ uS \\ 0 \end{bmatrix} = \begin{bmatrix} 0 \\ 0 \\ 0 \\ 0 \\ M_0 \\ 0 \end{bmatrix}, \qquad (11)$$

where $M_0 = uSC_{55}$ is the scalar moment. For $\mathbf{n}$ and $\mathbf{v}$ lying in the other symmetry planes, we obtain similar results. Hence, the shear sources situated in symmetry planes of orthorhombic anisotropy are represented by double couples similarly as in isotropic media, but they are scaled by different scalar moments:

$$\mathbf{M} = M_0 \begin{bmatrix} 0 & 1 & 0 \\ 1 & 0 & 0 \\ 0 & 0 & 0 \end{bmatrix}, \ M_0 = uSC_{66}, \ \text{ for } \mathbf{n} = \begin{bmatrix} 1 \\ 0 \\ 0 \end{bmatrix} \text{ and } \mathbf{v} = \begin{bmatrix} 0 \\ 1 \\ 0 \end{bmatrix}, \qquad (12)$$

$$\mathbf{M} = M_0 \begin{bmatrix} 0 & 0 & 1 \\ 0 & 0 & 0 \\ 1 & 0 & 0 \end{bmatrix}, \ M_0 = uSC_{55}, \ \text{ for } \mathbf{n} = \begin{bmatrix} 1 \\ 0 \\ 0 \end{bmatrix} \text{ and } \mathbf{v} = \begin{bmatrix} 0 \\ 0 \\ 1 \end{bmatrix}, \qquad (13)$$

$$\mathbf{M} = M_0 \begin{bmatrix} 0 & 0 & 0 \\ 0 & 0 & 1 \\ 0 & 1 & 0 \end{bmatrix}, \ M_0 = uSC_{44}, \ \text{ for } \mathbf{n} = \begin{bmatrix} 0 \\ 1 \\ 0 \end{bmatrix} \text{ and } \mathbf{v} = \begin{bmatrix} 0 \\ 0 \\ 1 \end{bmatrix}. \qquad (14)$$

Also we can derive conditions imposed on elastic parameters under which shear faulting in an anisotropic medium generates no ISO component. This happens if trace of $\mathbf{M}$ is zero (Jost & Hermann 1989). Equation (6) yields the following conditions for triclinic anisotropy

$$C_{16} + C_{26} + C_{36} = 0 \text{ , for } \mathbf{n} = \begin{bmatrix} 1 \\ 0 \\ 0 \end{bmatrix} \text{ and } \mathbf{v} = \begin{bmatrix} 0 \\ 1 \\ 0 \end{bmatrix} , \tag{15}$$

$$C_{15} + C_{25} + C_{35} = 0 \text{ , for } \mathbf{n} = \begin{bmatrix} 1 \\ 0 \\ 0 \end{bmatrix} \text{ and } \mathbf{v} = \begin{bmatrix} 0 \\ 1 \\ 0 \end{bmatrix} , \tag{16}$$

$$C_{14} + C_{24} + C_{34} = 0 \text{ , for } \mathbf{n} = \begin{bmatrix} 1 \\ 0 \\ 0 \end{bmatrix} \text{ and } \mathbf{v} = \begin{bmatrix} 0 \\ 1 \\ 0 \end{bmatrix} . \tag{17}$$

If we restrict anisotropy to generate no ISO component for any shear source with an arbitrary orientation, we obtain the following five conditions on 15 elastic parameters of triclinic anisotropy (see Appendix A):

$$C_{11} + C_{12} - C_{23} - C_{33} = 0 \ , \tag{18}$$

$$C_{11} + C_{13} - C_{22} - C_{23} = 0 \ , \tag{19}$$

$$C_{14} + C_{24} + C_{34} = 0 \ , \tag{20}$$

$$C_{15} + C_{25} + C_{35} = 0 \ , \tag{21}$$

$$C_{16} + C_{26} + C_{36} = 0 \ . \tag{22}$$

The five conditions (18-22) for triclinic anisotropy reduce to two conditions (18-19) for orthorhombic anisotropy and to only condition (18) for transverse isotropy. Interestingly, any cubic anisotropy satisfies eqs (18-22), hence no shear source can generate the ISO component in this symmetry.

2.2. Fault plane solutions

We distinguish two different coordinate systems for seismic sources in anisotropic media. The first coordinate system is defined by the eigenvectors of moment tensor **M**, which is related to stresses generated by a source. The other coordinate system is defined by eigenvectors of source tensor **D**, which is related to geometry of faulting. The both systems coincide in isotropy, but can differ in anisotropy. The deviation between them depends on symmetry and strength of anisotropy.

2.2.1. Eigenvectors of moment tensor **M**

The eigenvectors of the moment tensor **M** are called the P, T and B axes and define the coordinate system, in which the moment tensor **M** diagonalizes:

$$\mathbf{M}^{diag} = \begin{bmatrix} M_1 & 0 & 0 \\ 0 & M_2 & 0 \\ 0 & 0 & M_3 \end{bmatrix}, \text{ where } M_1 > M_2 > M_3 . \tag{23}$$

The P axis corresponds to the minimum eigenvalue M_3, the T axis corresponds to the maximum eigenvalue M_1, and the B axis corresponds to the intermediate eigenvalue M_2. Physically, the P, T and B axes define directions of the maximum compressional, maximum tensional and intermediate stresses generated by the source, respectively.

For isotropic media, the P, T and B axes can directly be inferred from the fault normal **n** and slip direction $\mathbf{v}$ as follows

$$\mathbf{b} = \mathbf{n} \otimes \mathbf{v} , \quad \mathbf{t} = \frac{\mathbf{n}+\mathbf{v}}{|\mathbf{n}+\mathbf{v}|} , \quad \mathbf{p} = \frac{\mathbf{n}-\mathbf{v}}{|\mathbf{n}-\mathbf{v}|} , \tag{24}$$

where **p**, **t** and **b** are unit vectors defining P, T and B axes, and symbol ⊗ denotes the vector product.

2.2.2. Eigenvectors of source tensor **D**

The source tensor **D**

$$\mathbf{D}=\frac{uS}{2}(\mathbf{nv}+\mathbf{vn})=\frac{uS}{2}\begin{bmatrix}2n_1\nu_1 & n_1\nu_2+n_2\nu_1 & n_1\nu_3+n_3\nu_1\\ n_1\nu_2+n_2\nu_1 & 2n_2\nu_2 & n_2\nu_3+n_3\nu_2\\ n_1\nu_3+n_3\nu_1 & n_2\nu_3+n_3\nu_2 & 2n_3\nu_3\end{bmatrix} \tag{25}$$

has the following diagonal form

$$\mathbf{D}^{diag}=\frac{uS}{2}\begin{bmatrix}\mathbf{n}\cdot\mathbf{v}+1 & 0 & 0\\ 0 & 0 & 0\\ 0 & 0 & \mathbf{n}\cdot\mathbf{v}-1\end{bmatrix}, \tag{26}$$

where $\mathbf{n}\cdot\mathbf{v}$ is the scalar product

$$\mathbf{n}\cdot\mathbf{v}=n_1\nu_1+n_2\nu_2+n_3\nu_3 \ . \tag{27}$$

The determinant of **D** is zero. The trace of **D** is $Tr(\mathbf{D})=uS\,(\mathbf{n}\cdot\mathbf{v})$. The maximum eigenvalue $D_1=\frac{uS}{2}(\mathbf{n}\cdot\mathbf{v}+1)$ is always positive, the minimum eigenvalue $D_3=\frac{uS}{2}(\mathbf{n}\cdot\mathbf{v}-1)$ is negative or zero. The eigenvectors $\mathbf{e}_1$, $\mathbf{e}_2$ and $\mathbf{e}_3$ of **D** are

$$\mathbf{e}_1=\frac{\mathbf{n}+\mathbf{v}}{|\mathbf{n}+\mathbf{v}|}\ ,\ \ \mathbf{e}_2=\mathbf{n}\otimes\mathbf{v}\,,\ \ \mathbf{e}_3=\frac{\mathbf{n}-\mathbf{v}}{|\mathbf{n}-\mathbf{v}|}\,. \tag{28}$$

Equation (28) applies to tensile sources (**n** and **ν** have arbitrary orientations) as well as to shear sources (**n** and **ν** are perpendicular).

2.2.3. Geometry of faulting

In order to determine fault normal **n** and slip direction **ν** from moment tensor **M** and from matrix of elastic parameters **C**, we have to calculate vector **d** from eq. (6)

$$\mathbf{d}=\mathbf{C}^{-1}\mathbf{m}\,, \tag{29}$$

and subsequently construct source tensor **D** using eq. (9). Diagonalizing **D**, we obtain eigenvalues D_1 and D_3, and eigenvectors $\mathbf{e}_1$, $\mathbf{e}_2$ and $\mathbf{e}_3$. The angle δ between the fault normal and slip direction is determined from the trace of **D** (see eq. (26))

$$\cos(\delta) = \frac{1}{uS}\,\mathrm{Tr}(\mathbf{D}) = \frac{D_1 + D_3}{D_1 - D_3} \; . \tag{30}$$

The fault normal **n** and slip direction $\boldsymbol{\nu}$ are determined from eigenvectors and eigenvalues of **D**:

$$\mathbf{n} = \frac{1}{\sqrt{D_1 - D_3}}\left(\sqrt{|D_1|}\,\mathbf{e}_1 + \sqrt{|D_3|}\,\mathbf{e}_3\right), \tag{31}$$

$$\boldsymbol{\nu} = \frac{1}{\sqrt{D_1 - D_3}}\left(\sqrt{|D_1|}\,\mathbf{e}_1 - \sqrt{|D_3|}\,\mathbf{e}_3\right). \tag{32}$$

For shear sources, $\mathrm{Tr}(\mathbf{D}) = 0$, $D_1 = \frac{uS}{2}$ and $D_3 = -\frac{uS}{2}$, hence

$$\mathbf{n} = \frac{1}{\sqrt{2}}\left(\mathbf{e}_1 + \mathbf{e}_3\right), \tag{33}$$

$$\boldsymbol{\nu} = \frac{1}{\sqrt{2}}\left(\mathbf{e}_1 - \mathbf{e}_3\right). \tag{34}$$

It follows from symmetry in positions of fault normal **n** and slip direction $\boldsymbol{\nu}$ in formulae (5) and (8) that the solution for **n** and $\boldsymbol{\nu}$ is ambiguous and the plus and minus signs in (31-32) and (33-34) can be interchanged.

3. Numerical modeling

3.1. Anisotropy models

In this section, we illustrate properties of moment tensors in anisotropic media numerically. We consider two transversely isotropic (TI) media, in which anisotropy is induced by presence of aligned cracks. In both models, the isotropic host rock was assumed to have the *P* and *S* velocities α = 4.5 km/s and β = 2.53 km/s and the density ρ = 2800 kg/m^3 typical of the uppermost crust.

Model A (see Shearer & Chapman 1989, Model 3) contains aligned, dry cracks with aspect ration 0.001 and cracks density 0.1. The symmetry axis of TI is along the x_3 – axis. Elastic parameters of the model are (in 10^9 kg m^{-1}s^{-2}):

$$\mathbf{C}^B = \begin{bmatrix} 53.31 & 17.78 & 12.32 & 0 & 0 & 0 \\ & 53.31 & 12.32 & 0 & 0 & 0 \\ & & 33.35 & 0 & 0 & 0 \\ & & & 14.28 & 0 & 0 \\ & & & & 14.28 & 0 \\ & & & & & 17.86 \end{bmatrix}. \quad (35)$$

Anisotropy of the P, SV and SH waves is 23.5%, 11.2% and 1.3%, respectively. The spatial variation of the phase velocities is shown in Fig. 1.

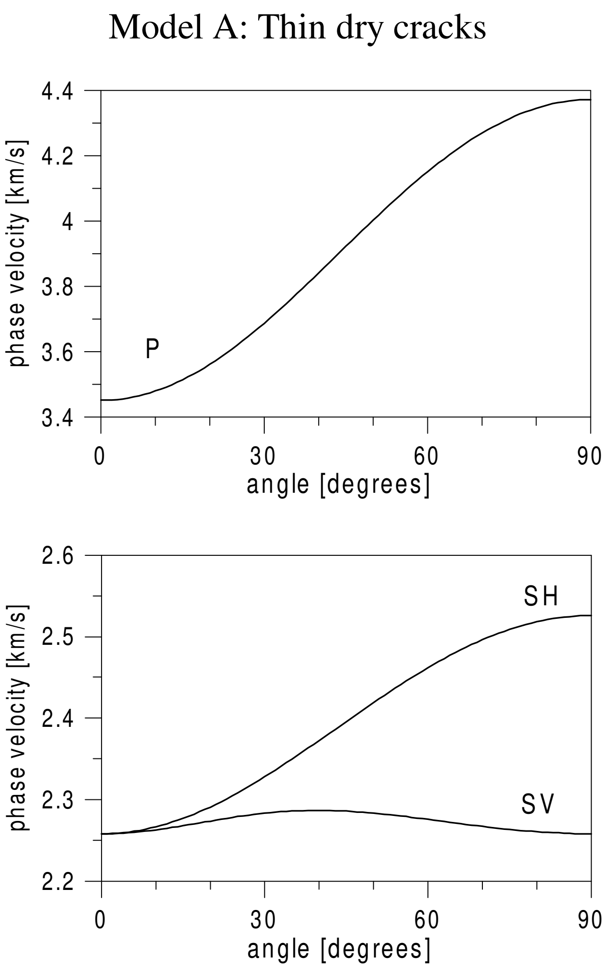

Fig. 1. Phase velocities for P (upper plot) and S (lower plot) waves as a function of the deviation of the wave normal from the symmetry axis for model A.

Model B (see Shearer & Chapman 1989, Model 1) contains aligned, water-filled cracks with aspect ratio 0.001 and crack density 0.1. The symmetry axis of TI is along the x_3 – axis. Elastic parameters of the model are (in 10^9 kg m^{-1}s^{-2}):

$$\mathbf{C}^A = \begin{bmatrix} 56.62 & 20.89 & 20.75 & 0 & 0 & 0 \\ & 56.62 & 20.75 & 0 & 0 & 0 \\ & & 56.11 & 0 & 0 & 0 \\ & & & 14.28 & 0 & 0 \\ & & & & 14.28 & 0 \\ & & & & & 17.86 \end{bmatrix}. \qquad (36)$$

Anisotropy of the *P*, *SV* and *SH* waves is 3.5%, 11.2% and 11.2%, respectively. The spatial variation of the phase velocities is shown in Fig. 2.

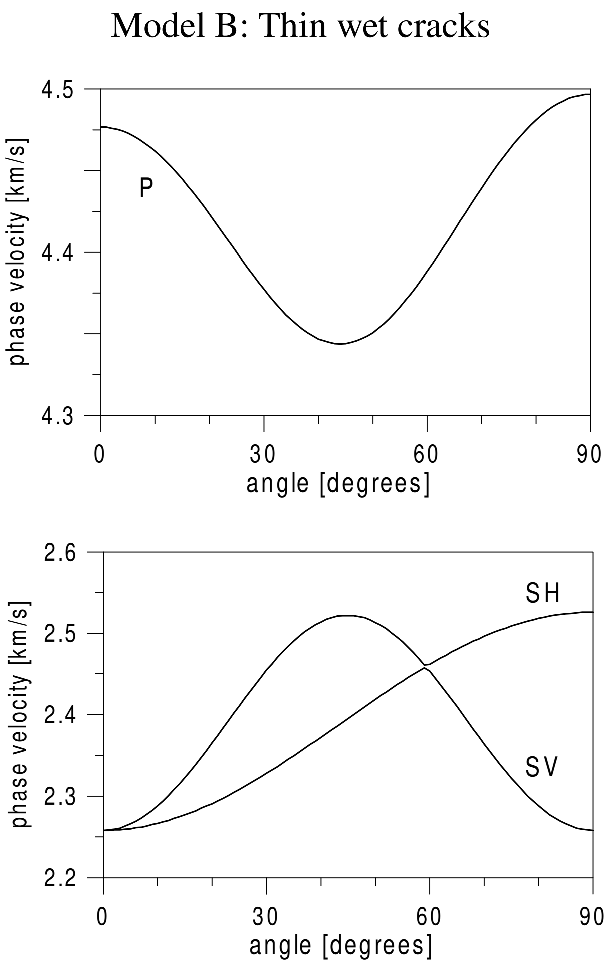

Fig. 2. Phase velocities for *P* (upper plot) and *S* (lower plot) waves as a function of the deviation of the wave normal from the symmetry axis for model B.

3.2. Non-DC components

Let us assume a shear source with the fault normal $\mathbf{n} = (0,0,1)^T$ and with the slip direction $\mathbf{v} = (1,0,0)^T$. Such source generates a moment tensor with no ISO and CLVD components for TI with the vertical symmetry axis. However, if the symmetry axis is inclined, the ISO and CLVD components become non zero. The DC and non-DC components of the moment tensor as a function of the direction of the symmetry axis are shown in Fig. 3 (model A) and in Fig. 4 (model B). For model A, the percentages of the ISO, CLVD and DC components range in the intervals: (–20.7, 20.7), (-16.1, 16.1) and (64.3, 100), respectively. For model B, the percentages of the ISO, CLVD and DC components range in the intervals: (–0.6, 0.6), (-19.9, 19.9) and (79.8, 100), respectively. Hence, the shear source produces remarkable non-DC components in both anisotropy models. In model A, both the ISO and CLVD are high. On the contrary, model B produces high CLVD, but almost zero ISO. Despite the different percentages of the ISO in both models, their spatial variation is similar. Interestingly, the spatial variations of the CLVD components are quite different for both models, the variation for model B being more complicated than for model A.

3.3. Correction for a true fault normal and slip direction

So far, fault plane solutions are calculated under the assumption of an isotropic focal area. If the focal area is anisotropic, the procedure yields distorted results. The errors owing to a neglect of anisotropy are shown in Fig. 5 (model A) and Fig. 6 (model B). The upper plots in the figures show the deviation between the true and approximated fault normals, the lower plots show the deviation between the true and approximated slip vectors. The approximate fault normal and the slip were calculated from the moment tensor as follows:

$$\mathbf{n}^{approx} = \frac{1}{\sqrt{2}}(\mathbf{p} + \mathbf{t}) , \tag{37}$$

$$\mathbf{v}^{approx} = \frac{1}{\sqrt{2}}(\mathbf{p} - \mathbf{t}) , \tag{38}$$

where $\mathbf{p}$ and $\mathbf{t}$ are the unit eigenvectors of the moment tensor corresponding to the P and T axes. Because of ambiguity of the solution (37-38) for the fault normal and slip, we selected that pair of $\mathbf{n}^{approx}$ and $\mathbf{v}^{approx}$ which better approximated the true vectors.

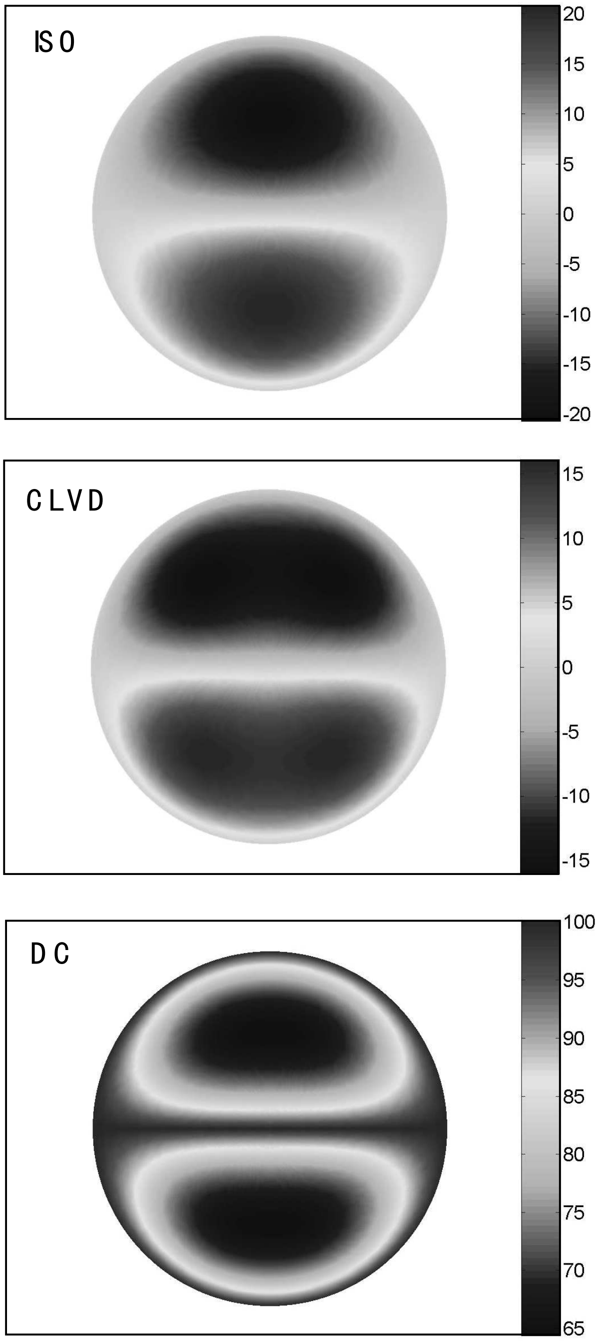

Fig. 3. The percentage of the DC and non-DC components of moment tensors generated by shear faulting in model A with the inclined symmetry axis. The percentage is calculated according to Vavryčuk (2001, Eqs 8a-8c). Equal-area projection is used.

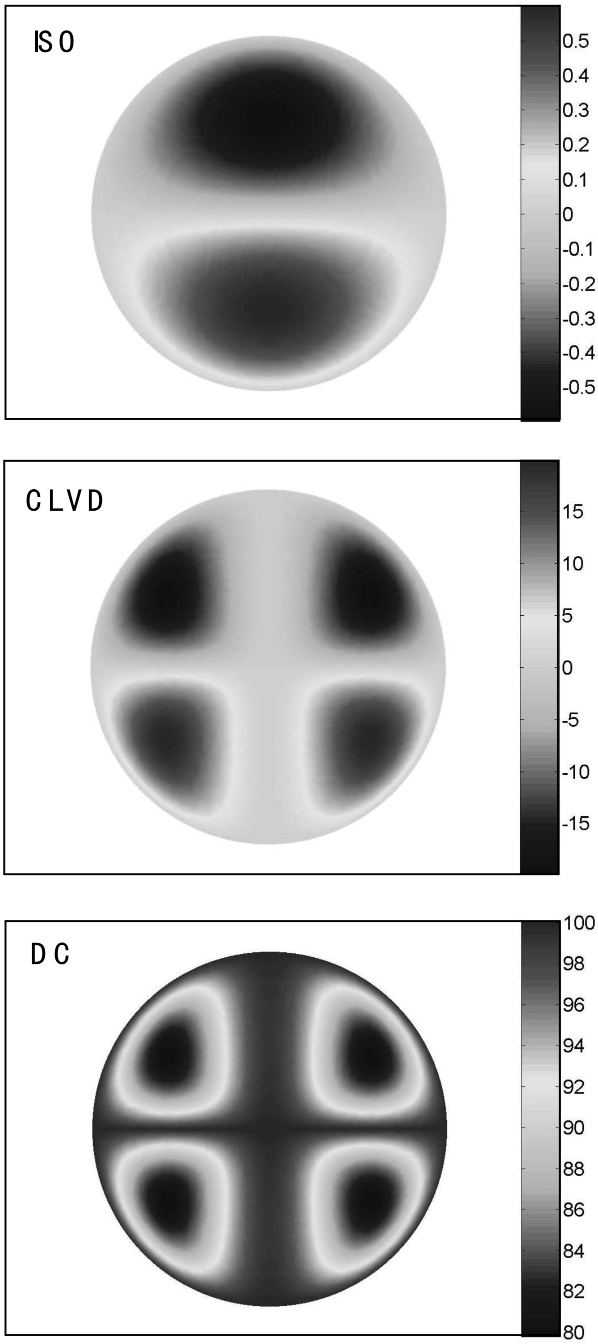

Fig. 4. The percentage of the DC and non-DC components of moment tensors generated by shear faulting in model B with the inclined symmetry axis. The percentage is calculated according to Vavryčuk (2001, Eqs 8a-8c). Equal-area projection is used.

Figures 5 and 6 show that the maximum deviation between true and approximated fault normals and true and approximated slips attains coincidently a value of 6.4°. This indicates that the deviation is not sensitive to strength of the *P*-wave anisotropy, which is different in models A and B, but only to strength of the *S*-wave anisotropy. The maximum deviation of 6.4°, corresponding to the *S*-wave anisotropy of 11.2%, is not very high, but still it can introduce a non-negligible bias in carefully determined focal mechanisms. Similarly as for the CLVD, the spatial variation of the deviations is more complicated for model B than for model A.

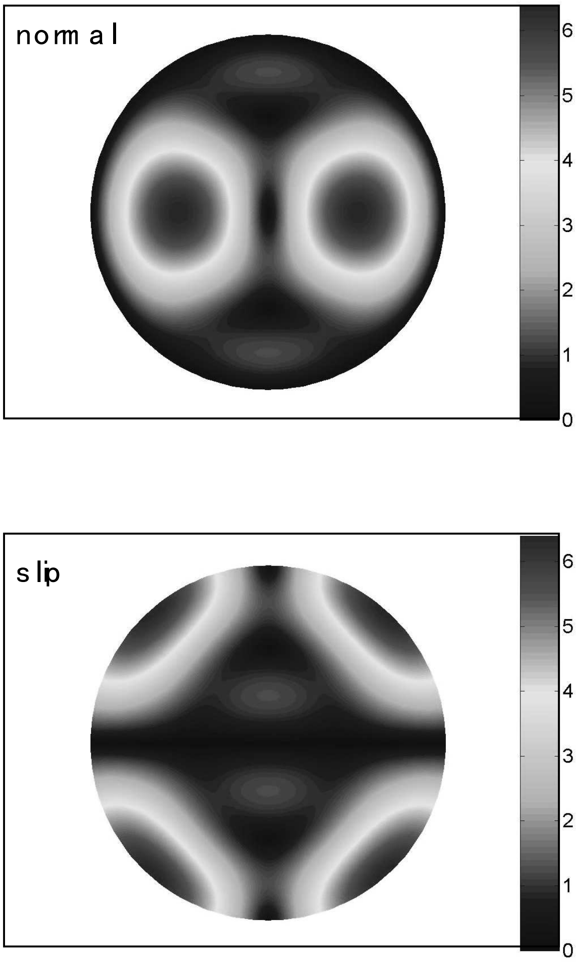

Fig. 5. The deviation between the true and approximated fault normals (upper plot), and between the true and approximated slip directions (lower plot) for model A. Equal-area projection is used. The deviation is in degrees.

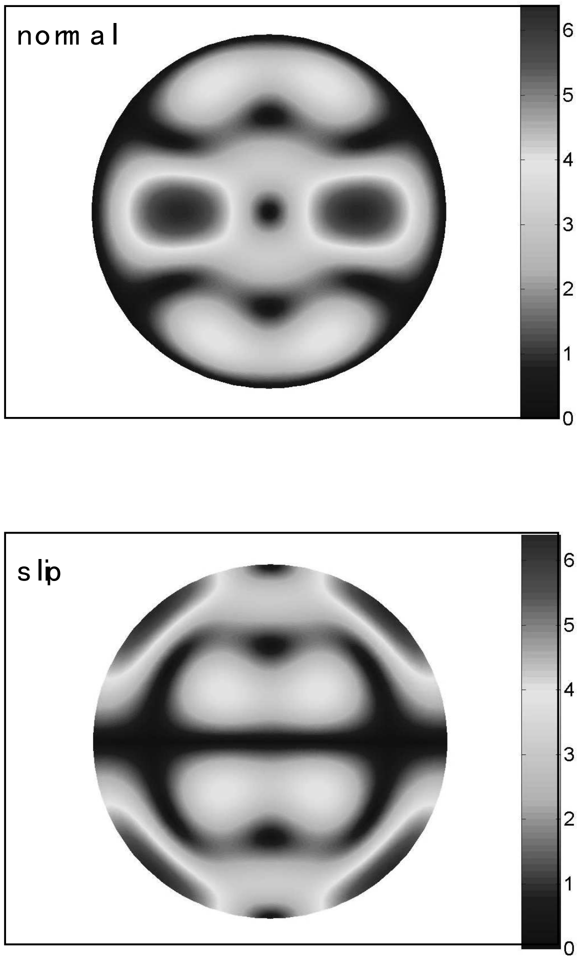

Fig. 6. The deviation between the true and approximated fault normals (upper plot), and between the true and approximated slip directions (lower plot) for model B. Equal-area projection is used. The deviation is in degrees.

4. Conclusions

(1) The moment tensors of planar shear sources in anisotropic media consist of DC but also of non-DC components. The non-DC components can comprise both the CLVD and ISO components. The amount of the CLVD and ISO varies and depends on the orientation, strength and symmetry of anisotropy.

(2) Under specific conditions imposed on anisotropy, shear sources with arbitrary orientations can generate no ISO components. These conditions are satisfied, for example, in cubic anisotropy. The ISO components produced by shear sources in triclinic anisotropy are not sensitive to parameters C_{44}, C_{45}, C_{46}, C_{55}, C_{56} and C_{66}.

(3) Shear sources generate no non-DC components, provided that shear faulting is situated in symmetry planes of orthorhombic or higher symmetries. In this case, shear faulting generates pure double-couple moment tensor similarly as in isotropic media, but the scalar seismic moment can vary with respect to the orientation of the slip in a symmetry plane.

(4) Geometry of faulting in anisotropy, i.e. the orientation of the fault normal and the slip direction, must be retrieved from moment tensors in a more complicated way than in isotropy. The P, T and B axes for shear sources in anisotropy are inclined from those in isotropy.

(5) Numerical modelling on media with aligned dry or water-filled penny shaped cracks with the crack density of 0.1 shows that shear faulting generates non-DC components with the percentage comparable with strength of anisotropy (~20%). The medium with water-filled cracks produces almost no ISO component for shear sources. The spatial variation of non-DC components depends on the type of cracks. This opens a possibility to retrieve different kinds of anisotropy by studying the non-DC components from a family of differently oriented shear sources.

(6) The deviation between the true fault normals and slip directions, and those approximately calculated by neglecting anisotropy attained 6° for the synthetic models. This indicates that the focal mechanisms are probably less sensitive to anisotropy than the percentages of the non-DC components.

Acknowledgments
The study was supported by the Grant Agency of the Academy of Sciences of the Czech Republic, Grant No. A3012309, by the Grant Agency of the Czech Republic, Grant No. 205/02/0383, and by the Consortium Project “Seismic waves in complex 3-D structures”..

References

Aki, K. & Richards, P.G., 2002. *Quantitative Seismology*. University Science Books, Sausalito, California.

Babuška, V. & Cara, M., 1991. *Seismic Anisotropy in the Earth*, Kluwer Academic Publisher, London.

Crampin, S., 1993. A review of the effects of crack geometry on wave propagation through aligned cracks, *Can. J. Expl. Geophysics*, **29**, 3-17.

Červený, V., 2001. *Seismic Ray Theory*, Cambridge University Press, Cambridge.

Frohlich, C., 1994. Earthquakes with non-double-couple mechanisms, *Science*, **264**, 804-809.

Helbig, K., 1994. *Foundations of Anisotropy for Exploration Seismics*, Pergamon, New York.

Jost, M.L. & Hermann, R.B., 1989. A student's guide to and review of moment tensors, *Seismol. Res. Lett.*, **60**, 37-57.

Julian, B.R., Miller, A.D. & Foulger, G.R., 1998. Non-double-couple earthquakes, 1. Theory, *Rev. Geophys.*, **36**, 525-549.

Kaneshima, S., Ando, M. & Kimura, S., 1988. Evidence from shear-wave splitting for the restriction of seismic anisotropy to the upper crust, *Nature*, **335**, 627-629.

Kawakatsu, H., 1991. Enigma of earthquakes at ridge-transform-fault plate boundaries – Distribution of non-double-couple parameter of Harvard CMT solutions, *Geophys. Res. Lett.*, **18**, 1103-1106.

Kawasaki, I. & Tanimoto, T., 1981. Radiation patterns of body waves due to the seismic dislocation occurring in an anisotropic source medium, *Bull. Seismol. Soc. Am.*, **71**, 37-50.

Kern, H. & Schmidt, R., 1990. Physical properties of KTB core samples at simulated in situ conditions, *Scientific Drilling*, **1**, 217-223.

Knopoff, L. & Randall, M.J., 1970. The compensated linear vector dipole: A possible mechanism for deep earthquakes, *J. Geophys. Res.*, **75**, 4957-4963.

Miller, A.D., Foulger, G.R. & Julian, B.R., 1998. Non-double-couple earthquakes, 2. Observations, *Rev. Geophys.*, **36**, 551-568.

Kuge, K. & Kawakatsu, H., 1992. Deep and intermediate depth non-double couple earthquakes – Interpretation of moment tensor inversions using various passbands of very broad-band seismic waves, *Geophys. J. Int.*, **111**, 589-606.

Kuge, K. & Lay, T., 1994. Systematic non-double-couple components of earthquake mechanisms: The role of fault zone irregularity, *J. Geophys. Res.*, **99**, 15.457-15.467.

Lay, T. & Wallace, T.C., 1995. *Modern Global Seismology*, Academic Press, New York.

Mainprice, D., Barruol, G. & Ben Ismail, W., 2000. The seismic anisotropy of the Earth's mantle: From single crystal to polycrystal, In: *Earth's Deep Interior, Mineral Physics and Tomography from the Atomic to the Global Scale* (Karato, S., Forte, A., Liebermann, R.C., Masters, G. & Stixrude, L., eds), Geophysical Monograph Series, American Geophysical Union, Washington, 237-264.

Musgrave, M.J.P., *Crystal Acoustics*, Holden Day, San Francisco, 1970.

Pros, Z., Lokajíček, T. & Klíma, K., Laboratory approach to the study of elastic anisotropy on rock samples, *Pure Appl. Geophys*., **151**, 619-629.

Rabbel, W. & Mooney, W.D., 1996. Seismic anisotropy of the crystalline crust: What does it tell us?, *Terra Nova*, **8**, 16-21.

Rössler, D., Rümpker, G. & Krüger, F., 2003. Ambiguous moment tensors and radiation patterns in anisotropic media with applications to the modeling of earthquake mechanisms in W-Bohemia, *Stud. Geophys. Geod.*, **48**, 233-250.

Savage, M.K., 1999. Seismic anisotropy and mantle deformation: What have we learned from shear wave splitting? *Rev. Geophysics*, **37**, 65-106.

Shearer, P.M. & Chapman, C.H., 1989. Ray tracing in azimuthally anisotropic media – I. Results for models of aligned cracks in the upper crust, *Geophys. J. Int.*, **96**, 51-64.

Silver, P.G., 1996. Seismic anisotropy beneath the continents: Probing the depths of geology, *Ann. Rev. Earth Planet. Sci.*, **24**, 385-432.

Sipkin, S.A., 1986. Interpretation of non-double-couple earthquake mechanisms derived from moment tensor inversion, *J. Geophys. Res.*, **91**, 531-547.

Vavryčuk, V., 2001. Inversion for parameters of tensile earthquakes, *J. Geophys. Res.*, **106**, 16.339-16.355.

Vavryčuk, V., 2002. Non-double-couple earthquakes of 1997 January in West Bohemia, Czech Republic: Evidence of tensile faulting, *Geophys. J. Int*., **149**, 364-373.

Appendix A: Anisotropy generating no ISO components for shear faulting with an arbitrary orientation

Suppose a shear source in triclinic anisotropy with fault normal $\mathbf{n} = (0,0,1)^T$ and slip direction $\mathbf{v} = (1,0,0)^T$. According to eq. (10), the moment tensor of the source is expressed as follows:

$$\mathbf{M} = uS \begin{bmatrix} C^*_{15} & C^*_{56} & C^*_{55} \\ & C^*_{25} & C^*_{45} \\ & & C^*_{35} \end{bmatrix} . \tag{A1}$$

The zero ISO components is equivalent to the condition of zero trace of **M**

$$Tr(\mathbf{M}) = uS\left(C^*_{15} + C^*_{25} + C^*_{35}\right) = 0 \ , \tag{A2}$$

where matrix of elastic parameters $\mathbf{C}^*$ is evaluated in the coordinate system, in which two axes (x_1 and x_3) are formed by vectors **n** and $\mathbf{v}$. For an arbitrary orientation of the coordinate system with respect to the orientation of shear faulting, the elasticity tensor c_{ijkl} must be rotated (see Musgrave 1970, eq. 3.12.2a). Using the following rotated coordinate system

$$\mathbf{e}_1 = \begin{bmatrix} -\sin\psi\sin\varphi\cos\theta + \cos\psi\cos\varphi \\ -\sin\psi\cos\varphi\cos\theta - \cos\psi\sin\varphi \\ \sin\psi\sin\theta \end{bmatrix} , \tag{A3}$$

$$\mathbf{e}_2 = \begin{bmatrix} \sin\psi\cos\varphi + \cos\psi\sin\varphi\cos\theta \\ -\sin\psi\sin\varphi + \cos\psi\cos\varphi\cos\theta \\ -\cos\psi\sin\theta \end{bmatrix} , \tag{A4}$$

$$\mathbf{e}_3 = \begin{bmatrix} \sin\varphi\sin\theta \\ \cos\varphi\sin\theta \\ \cos\theta \end{bmatrix} . \tag{A5}$$

where ψ, φ and θ are arbitrary angles, the trace of **M** reads

$$
\begin{aligned}
\mathrm{Tr}(\mathbf{M}) = {} & uS(C_{11}+C_{12}-C_{23}-C_{33})\sin\varphi\sin\theta\cos\theta \\
& - uS(C_{11}+C_{13}-C_{22}-C_{23})\cos\psi\sin\theta\,(\sin\psi\cos\varphi+\cos\psi\sin\varphi\cos\theta) \\
& - uS(C_{14}+C_{24}+C_{34})(\sin\psi\cos\varphi\cos\theta+\cos\psi\sin\varphi\cos 2\theta) \\
& - uS(C_{15}+C_{25}+C_{35})(\cos\psi\cos\varphi\cos\theta-\sin\psi\sin\varphi\cos 2\theta) \\
& - uS(C_{16}+C_{26}+C_{36})\left(\frac{1}{2}\sin 2\psi\sin\varphi\sin 2\theta-\cos 2\psi\cos\varphi\sin\theta\right).
\end{aligned}
\tag{A6}
$$

The condition of zero trace of **M** for any value of angles ψ, φ and θ yields

$$C_{11}+C_{12}-C_{23}-C_{33}=0 \ , \tag{A7}$$

$$C_{11}+C_{13}-C_{22}-C_{23}=0 \ , \tag{A8}$$

$$C_{14}+C_{24}+C_{34}=0 \ , \tag{A9}$$

$$C_{15}+C_{25}+C_{35}=0 \ , \tag{A10}$$

$$C_{16}+C_{26}+C_{36}=0 \ . \tag{A11}$$

Equations (A7-A11) represent a system of five equations for 15 elastic parameters of triclinic anisotropy. Since parameters C_{44}, C_{45}, C_{46}, C_{55}, C_{56} and C_{66} are missing in the equations, we conclude that the ISO component is not sensitive to them.